

Interlayer coupling in Co/Si sandwich structures

J. Enkovaara, A. Ayuela, and R. M. Nieminen

Laboratory of Physics, Helsinki University of Technology, 02015 Espoo, Finland

(Received 6 March 2000; revised manuscript received 1 August 2000)

The combinations of magnetic materials with traditional semiconductors are interesting possibilities for new magnetoresistive structures. In this work the interlayer magnetic coupling in Co-Si systems has been studied. The coupling has been calculated within the density-functional theory, and it has been observed to oscillate with a spatial period of two Si layers. The electronic structure analysis indicates the formation of quantum wells within the Si spacer.

I. INTRODUCTION

Traditional electronics is based on the electron charge, while another fundamental property of the electron is its spin. The exploitation of the spin in carrier transport moves one from the era of electronics to the era of magnetoelectronics (“spintronics”). In layered structures, where ferromagnetic layers are separated by nonmagnetic spacer layers, the electron spin has significant consequences. An external magnetic field may produce changes of up to $\sim 100\%$ in the resistivity—a phenomenon called giant magnetoresistivity (GMR). GMR was observed in 1988 in layered structures with nonmagnetic metallic spacers.^{1,2} The GMR effect oscillates as the thickness of the nonferromagnetic spacer layers between the spacer layers is increased. This oscillation is shown to be caused by an oscillation in the sign of interlayer exchange coupling (IEC) between the ferromagnetic layers.³ The net magnetic coupling between ferromagnetic films varies from ferromagnetic to antiferromagnetic as the spacer film thickness is varied.

Even though large GMR effects have been found in many structures, research is active for new material alternatives. One interesting possibility is the combination of magnetic materials with materials used in contemporary electronics. Cobalt has been used in many GMR structures, and silicon is without a doubt the most important material of modern electronics. It is therefore natural to consider multilayer structures based on Co and Si.

Some experiments have been performed for the transition-metal/Si multilayers grown by ion-beam sputtering techniques. In Co/Si multilayers, the coupling is found to be ferromagnetic below nominal Si layer thickness of 8 Å, antiferromagnetic between 8 and 17 Å, and the coupling disappears above 17 Å.⁴ Similar behavior has been found also in Fe/Si multilayers, where the coupling is ferromagnetic below Si thickness of 10 Å, then changes to antiferromagnetic and finally vanishes above 20 Å.⁵

For Fe/Si multilayers, the antiferromagnetic interlayer coupling between the Fe films was associated with a spacer consisting of metallic, crystalline iron silicide.^{6,7} The absence of coupling was ascribed to amorphous Si. The analysis of the magnetic coupling and the magnetoresistance of transition-metal/Si layers seems to be difficult due to the lack of detailed knowledge about the structure and composition of the spacer film. To clarify the situation, first-principles cal-

culations for well-defined structures can be helpful.

In this paper we report studies of ideal Co/Si multilayers using *ab initio* calculations and a supercell technique. The interlayer coupling in this system is studied using the full-potential linearized augmented plane-wave (FLAPW) method⁸ within the density-functional theory. First, some computational details and a discussion of the structures are given in Sec. II. The results in Sec. III include the interlayer coupling and the overall magnetic properties. We found that the interlayer coupling oscillate with two Si layers. This is analyzed in terms of the calculated electronic structure. Section IV summarizes the conclusions.

II. COMPUTATIONAL DETAILS

A. Method

The calculations are done within the density-functional theory using the FLAPW method as implemented in the WIEN97 code.⁸ The FLAPW method is among the most accurate band-structure methods presently available. The exchange-correlation potential is approximated by the generalized-gradient approximation (GGA) of Perdew *et al.*⁹ The muffin-tin radii are 1.218 Å for Co and 1.138 Å for Si. The maximum value in the radial sphere expansion is $l_{max}=10$, and the largest l value for the non-spherical part of the Hamiltonian matrix is $l_{max,ns}=4$. The cutoff parameters are $RK_{max}=9$ for the plane waves and $RG_{max}=14$ for the charge density, so that no shape approximation to the potential occurs. The number of plane waves ranges from 729 to 1560, depending on the number of Si layers. Brillouin-zone integrations are weighted by special points generated with the improved tetrahedron method, where a Fermi broadening of 0.002 Ry is used. As the number of k points is varying through the paper, the convergence of the integration is discussed later. The core electrons are treated fully relativistically while the valence electrons are treated as scalar relativistic.

B. Structural comments

The magnetic Co thin films develop a hcp structure as is shown in Ref. 4. The Co film is modeled here mainly by two Co layers (0001). In this work the Si layers for small Si film thickness are assumed to grow also in the hcp structure with ideal interfaces, without interdiffusion. This assumption is

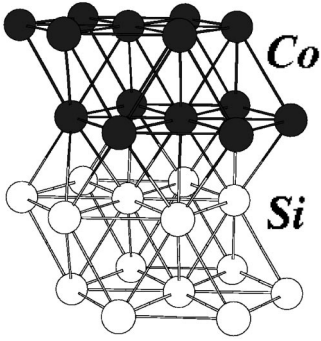


FIG. 1. Unit cell with two Si layers.

justified later on the basis of the electronic origin for the coupling. The unit cell for Co_2/Si_2 is shown in Fig. 1.

The input structure has been chosen with the atomic positions as in bulk Co, with an interlayer distance of 2.04 Å. The hexagonal lattice constant is $a = 2.68$ Å. The total energy is converged within 0.1 mRy with respect to the number of \vec{k} points, where 64 \vec{k} points in the irreducible Brillouin zone are used. Then the structure with two Si layers is optimized with respect to the inner lattice parameters, the unit-cell volume, and the c/a ratio, in this order. The lattice parameters after these optimizations are given in Table I.

The distance between the Co layers stays almost unchanged in its bulk value, while the distance between Si layers increases and the interface distance between the Co and Si layers decreases. The structure of the spacer is close to the structure of bulk hcp Si, where $a = 2.68$ Å and $d_{\text{Si-Si}} = 2.28$ Å.¹⁰ The nearest-neighbor distance between Co and Si is 2.36 Å, close to the calculated one for the CoSi_2 silicide 2.32 Å.¹¹ In the calculations for larger systems, e.g., for Co_2/Si_n layers with $n = 3-6$, the distances between layers have the values from the relaxed structure with two Si layers.

C. Magnetic coupling and k -point convergence

For the spacer thicknesses considered here the magnetic coupling energy ΔE can be obtained as the total-energy difference between the ferromagnetic and antiferromagnetic alignments of the Co layers. The unit cell has to be doubled, so that the magnetic configuration in the adjacent Co_2 films can be different. The charge oscillations in the self-consistency cycles are avoided by using small mixing parameters, $\alpha \leq 0.01$, which makes the convergence of the calculations slow.

The total-energy convergence with respect to \vec{k} sampling has been checked, e.g., the number of \vec{k} -points in the irreducible Brillouin zone for Co_2/Si_2 is 121 both in the antiferromagnetic and ferromagnetic configuration. The magnetic coupling ΔE for $n > 2$ converges faster than the total energy

TABLE I. Optimized lattice parameters and distances between the layers in Å.

a	c	$d_{\text{Co-Co}}$	$d_{\text{Si-Si}}$	$d_{\text{Co-Si}}$
2.64	7.90	2.02	2.25	1.80

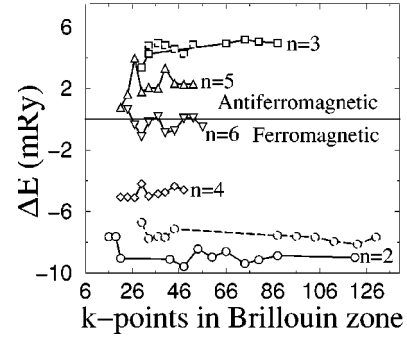


FIG. 2. Total-energy differences ΔE with respect to the number of \vec{k} points for different number n of Si layers. The full line and marks are for Co_2Si_n ; the dotted line and marks are for Co_4Si_n .

as a function of the number of \vec{k} points, as is shown in Fig. 2 for Co_2/Si_n with $n = 2-6$. The energy difference is converged for $n = 2-5$ Si layers. On the other hand, the convergence for $n = 6$ is not clear because the sign of exchange coupling could be uncertain when increasing the number of \vec{k} points, as ΔE is close to zero. The exchange coupling for Co_4/Si_n with $n = 2, 3$ is also plotted in Fig. 2. Although \vec{k} -point convergence is not clear, the sign of the coupling is already given. The energy difference between Co_2Si_2 and Co_4Si_2 is smaller than the one between Co_2Si_2 and Co_2Si_4 . In any case, the Co_2Si_3 and Co_4Si_3 cases have the same value. When increasing the number of Co layers, it seems that the sign of the coupling is not going to change. In the following, we limit our discussion to the Co_2Si_n results.

III. RESULTS

A. Exchange coupling and magnetic properties

The exchange coupling when varying the number of Si layers is shown in Fig. 3. The coupling oscillates from ferromagnetic to antiferromagnetic with a period of two Si layers. For Co_2Si_n there is an asymmetric component that seems to favor the ferromagnetic coupling. A larger thickness of the Co film does not change the alternating behavior of the coupling, as seen in Fig. 2. The calculated oscillatory interlayer coupling is not evident in the experiments.⁴ However, sev-

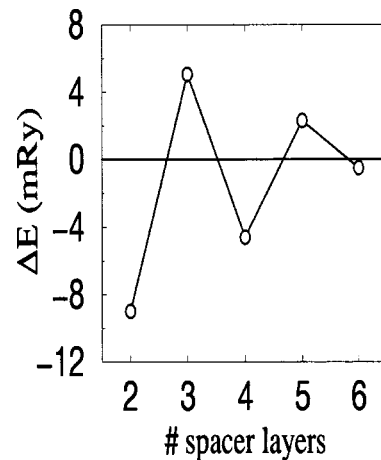


FIG. 3. Calculated exchange coupling with the number of Si layers for Co_2Si_n .

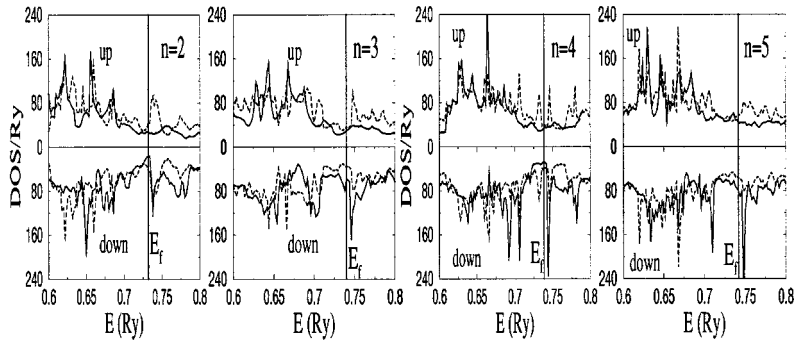


FIG. 4. DOS around the Fermi level for Co_2/Si_n . Full line, ferromagnetic configuration; dotted line, antiferromagnetic configuration.

eral spacer differences that can affect the coupling appear to explain this inconsistency: (i) silicide formation, (ii) a different geometry, and (iii) interface roughness which affects especially the small-period oscillations. These arguments, especially (i) and (iii) will receive further reinforcement later in this work.

The magnetic properties of the Co layers are affected by the presence of the Si layers. The magnetic moments in the Co atomic sphere range between $1.01\mu_B$ and $1.09\mu_B$. The moments are smaller than the magnetic moment in bulk Co ($1.6\mu_B$). If one considers the decrease in the magnetic moment of Co due the decrease in the number of Co neighbors from 12 to 9 in a linear fashion, a slightly larger value of $9/12 \times 1.6\mu_B = 1.2\mu_B$ is obtained. This magnetic reduction is explained by a charge redistribution from the spin-down electrons to the spin-up component inside the Co sphere. The Si atomic spheres have also small magnetic moments, $\mu_{\text{Si}} < 0.05\mu_B$. The magnetic configuration with a lower energy shows a larger magnetic moment in the interfacial Si layer, but for Co there is no such clear trend. This is studied in more detail in the next section.

B. Electronic structure

The reversal of the coupling is directly related to the density of states (DOS) around the Fermi level. The DOS for Co_2/Si_n are shown in Fig. 4 between 0.6 and 0.8 Ry. For both spin-up and spin-down electrons, the DOS near the Fermi level with an even number of Si layers is smaller in the ferromagnetic configuration than in the antiferromagnetic configuration. With three Si layers the spin-up DOS is slightly larger in the antiferromagnetic configuration, but the spin-down DOS is smaller, and the difference is clearly larger than in the spin-up DOS. With five Si layers, the spin-up DOS is nearly equal for both magnetic configurations, but the spin-down DOS is smaller in the antiferromagnetic configuration. The configuration with the smaller DOS near the Fermi level seems to have the smaller total energy, and is thus the ground state.

The states near the Fermi level also determine the transport properties of the structure. The layerwise decomposed DOS at the Fermi level (FDOS) has been studied in more detail. FDOS in the atomic spheres for $n=2-5$ in the ferromagnetic configuration (the antiferromagnetic case follows similar behavior) is shown in Fig. 5. In all cases the FDOS for spin-up electrons is about the same, but for an odd number of layers the spin-down FDOS is about three times as large as the spin up FDOS . The up-down spin symmetry in the Co interface for even n is in agreement with the favoring

of the ferromagnetic solution in the quantum interference model.¹² A large spin asymmetry in the FDOS of the ferromagnetic interface is correlated with a large spin-conduction asymmetry. Therefore the asymmetric FDOS for the odd Si layer number would indicate the possibility of the GMR.

The Co films induce modifications in the spacer layers for the magnetic state under consideration. Although the DOS difference between the ferromagnetic and antiferromagnetic configuration is largest within the Co sphere, the effect can be also seen in the Si spheres. To gain more insight, the projected DOS in the Si atomic spheres has been investigated. As an interesting feature, the Si projected DOS does not show a gap at E_f . While the absence of a gap is partly due to the assumed hcp structure of Si layers, the effect seems to be general in metal/semiconductor multilayers. Calculations for Fe/Ge, Fe/GaAs,¹³ and Fe/ZnSe,¹⁴ multilayers show no gap in the DOS when the number of spacer layers increases up to a maximum of nine for the Ge and GaAs spacers, and up to 33 for the ZnSe. Also, calculations for CoSi_2/Si interfaces¹⁵ show no gap for the first two Si layers near the interface.

Because the higher magnetic moment within the Si spheres is correlated with the ground-state magnetic configura-

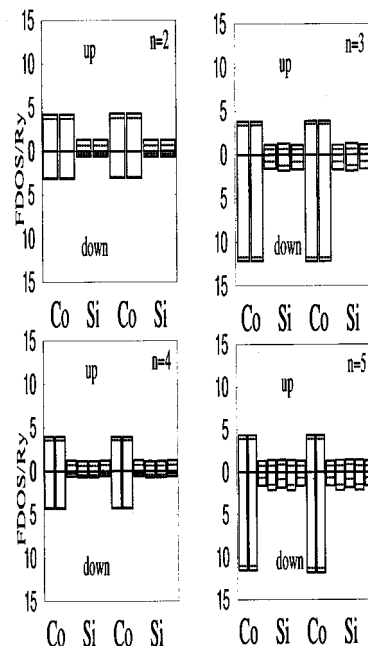


FIG. 5. DOS at the Fermi level in the atomic spheres for the ferromagnetic configuration. The part of the angular momentum projected DOS is also given by the dotted line: d in Co, p in Si.

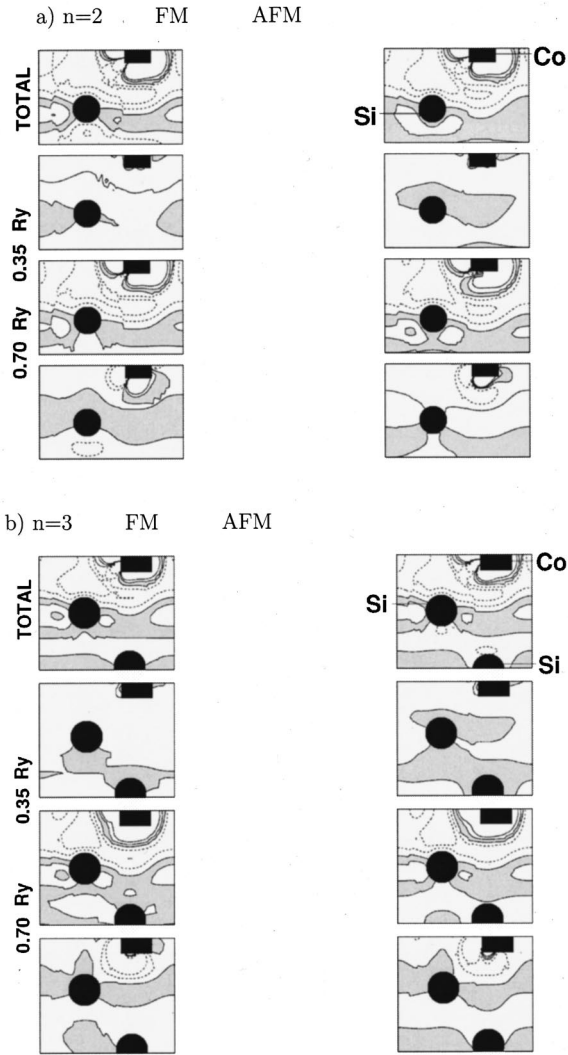


FIG. 6. Spin densities in the $(\bar{1}20)$ plane for (a) Co_2Si_2 and (b) Co_2Si_3 . First row, total spin densities; second to fourth, the three energy windows separated by the energies 0.35 Ry, 0.7 Ry and Fermi level (≈ 0.73 Ry). Contours are separated by $0.005e/\text{\AA}^3$. Solid contours denote positive spin (up) polarization and dashed lines denote negative spin polarization.

ration, the spin polarization in the Si spacer has been analyzed. In addition, for other systems photoemission spectroscopy experiments as well as *ab initio* calculations indicate also that the states relevant to coupling are spin polarized in the spacer.¹⁶ The spin density has been studied in three energy windows, where the first one is at low energies with a small spin density, the second is the region of the Co *d* electrons which has the largest spin density, and the third is the region near the Fermi level. The contour plots of the spin density for the ferromagnetic and antiferromagnetic configuration for $n=2-3$ are shown in Fig. 6. The spin density in the Si layers for the case of even (odd) Si layers is larger in the ferromagnetic (antiferromagnetic) than in the antiferromagnetic (ferromagnetic) configuration. For n fixed, the configuration with a larger spin density in the Si layers has the smaller energy. Spatially, most of the Si *sp* state magnetization resides near the interface where hybridization with the magnetic Co states is strongest (see the middle window be-

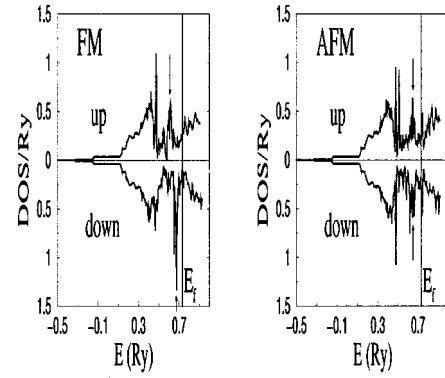


FIG. 7. p_z density of states within the interfacial Si layers for Co_2Si_2 .

tween 0.35 and 0.7 Ry). For the lowest-energy configuration, the electrons with an energy between 0.7 Ry and E_f also show the main topology as the total density polarization in the middle of the Si spacer.

The spin polarization in the Si spacer layers is carried by *sp* bands around E_f . On the other hand, the polarization induced in the Si orbitals by the magnetic Co atoms is p_z -like as seen in the ferromagnetic case of Fig. 6(a). The interaction between the Co layers is also transmitted mostly by the Si p_z electrons. Here, the p_z DOS in the interfacial Si layer is only shown for $n=2$ in Fig. 7. In the low-energy region, the two-dimensional states are shown clearly as a staircase structure. In the energy region up to the Fermi energy the peak structure in the antiferromagnetic configuration corresponds to an average of the ferromagnetic configuration (see the arrows in Fig. 7). Near the Fermi level the configuration with a lower energy has a lower p_z DOS like the total DOS. For $n=2$ there is a peak in the antiferromagnetic DOS just above the Fermi level (see Fig. 7), and for $n=4$ a similar peak is shown just below the Fermi level. However no such peaks are seen for $n=3$ and 5.

The two-dimensional DOS indicates the presence of quantum wells in the structure. The development of the quantum-well states in the low-energy region and the movement of the peaks in the middle-energy region suggest that the behavior of the states near the Fermi level could be described qualitatively with a simple quantum-well model. The states at the bottom of the well are similar for both spins and for both magnetic configurations, but in the higher energies the situation is different. Because the edges of the well are determined by the magnetic Co atoms, the spin-up and spin-down states have different energy in the ferromagnetic configuration. In the antiferromagnetic configuration the states are the same for both spins and they can be thought as an average of the ferromagnetic states. When the number of Si layers is changed, some quantum-well states develop through the Co *d* states. Depending on the number of Si layers, there are either ferromagnetic or antiferromagnetic states below the Fermi level, and the states of the other magnetic configuration have lower energy. The well states near the Fermi level hybridize with the Co *d* states, affecting also the Co DOS. The states of the stable magnetic configuration are in the energy region around E_f , where the magnetic interactions are stronger and the spin density is therefore larger.

As the quantum-well model describes the overall electronic structure, a Si spacer with a diamond structure should also show the two-layer oscillatory exchange coupling. Because the absence of the band gap seems to be a general trend in the transition-metal/semiconductor multilayers, there should be some states at the Fermi level in the diamond structure and the well states should also develop. The thickness of the Co layers should not affect the sign of the coupling energy in the above model either. This would leave the interface roughness and the silicide formation in the spacer as the more plausible reasons for the inconsistency between our calculations and the experimental results as has already been mentioned.

IV. CONCLUSIONS

As the combination of magnetic materials with traditional electronics materials for new GMR structures is interesting, Co/Si multilayers have been studied in this work. The interlayer coupling has been calculated within the density-functional theory, and it is found to oscillate between ferromagnetic and antiferromagnetic cases with the number of Si layers. The oscillation period behavior is found to be two atomic layers. Experimentally, such ideal oscillatory coupling has not been found. The experimentally observed cou-

pling with increasing Si thickness is first ferromagnetic, then antiferromagnetic, and finally it vanishes.

The electronic structure of the multilayers has been analyzed to gain insight into the calculated coupling. The lower-energy state has been found to correlate with the larger spin polarization within the Si layers and with the lower density of states near the Fermi level. The development of the two-dimensional electronic states suggests that the formation of quantum well states describes the coupling. On the other hand, a large spin asymmetry is observed near the Fermi level in the structures with three and five Si layers, indicating the possibility for asymmetry in the spin conduction, and therefore also the possibility for GMR.

The quantum-well model suggests that the interface roughness and the formation of silicide in the spacer would be the main reasons for the discrepancy between calculations and experiment. The interface roughness is difficult to study with the methods used in this work, but future work is planned for structures with silicide spacers.

ACKNOWLEDGMENTS

A. Ayuela was supported by the EU TMR program (Contract No. ERB4001GT954586).

¹M.N. Baibich *et al.*, Phys. Rev. Lett. **61**, 2472 (1988).

²G. Binasch, P. Grünberg, F. Saurenbach, and W. Zinn, Phys. Rev. B **39**, 4828 (1989).

³S.S. Parkin, IBM J. Res. Dev. **42**, 3 (1998) and references therein.

⁴K. Inomata and Y. Saito, J. Appl. Phys. **81**, 5344 (1997).

⁵Y. Endo, O. Kitakami, and Y. Shimada, Phys. Rev. B **59**, 4279 (1999).

⁶A. Chaiken, R.P. Michel, and M.A. Wall, Phys. Rev. B **53**, 5518 (1996).

⁷J.A. Carlisle *et al.*, Phys. Rev. B **53**, R8824 (1996).

⁸P. Blaha, K. Schwarz, and J. Luitz, WIEN97, Vienna University of Technology, 1997 (An improved and updated Unix version of the copyrighted WIEN code, which was published by P. Blaha, K. Schwarz, P. Sorantin, and S.B. Trickey, Comput. Phys. Commun. **59**, 399 (1990)).

⁹J. Perdew, K. Burke, and M. Ernzerhof, Phys. Rev. Lett. **77**, 3865 (1996).

¹⁰Our calculation using the same computational parameters and optimizing the volume and c/a ratio.

¹¹E.G. Moroni, R. Podloucky, and J. Hafner, Phys. Rev. Lett. **81**, 1969 (1998).

¹²P. Bruno, *Magnetische Schichtsysteme*, edited by P.H. Dederichs and P. Grünberg (Forschungszentrum, Jülich, 1999).

¹³W.H. Butler *et al.*, J. Appl. Phys. **81**, 5518 (1997).

¹⁴J.M. MacLaren, X.-G. Zhang, W.H. Butler, and X. Wang, Phys. Rev. B **59**, 5470 (1999).

¹⁵H. Fujitani and S. Asano, Phys. Rev. B **50**, 8681 (1994).

¹⁶R. Kläsger *et al.*, Phys. Rev. B **57**, R696 (1998), and references therein.